Electronic Materials Letters, Vol. 6, No. 1 (2010), pp. 7-12
DOI: 10.3365/eml.2010.03.007 Published 31 March 2010

Fabrication and Sensing Properties of a Micro-Humidity Sensor System Using CMOS Technology

Sung Pil Lee*

Department of Electronic Engineering, Kyungnam University, Masan, 631-701 Korea

A micro-humidity sensor system is designed and fabricated by 0.8 μm analog mixed CMOS technology. The integrated sensor system consists of an n-channel differential FET humidity sensor, a Wheatstone bridge humidity senor, and an operational amplifier block, respectively. The differential sensor employs carbon nitride films as a new sensing material and has a pair of transistors, a sensing transistor and a non-sensing transistor (reference transistor), to eliminate unexpected effects. The drain current of the FET humidity sensor increases from 0.88 mA to 0.99 mA as the relative humidity increases from 10 %RH to 70 %RH.

Keywords: micro humidity sensor, CMOS, carbon nitride, OP amp

1. INTRODUCTION

Sensors are critical for many products and systems. To some extent, however, the development of sensors has not keep pace with the rapid development of microelectronic components. For this reason, sensorics is in a restructuring phase in the direction of achieving increased miniaturization and integration of sensors and signal processing within a total system. This is lending substantially more importance to technologies that permit low-cost manufacture of both sensors and related electronics.[1]

Semiconductor chemical sensors, where semiconductor materials are mainly responsible for the sensor operation and/or semiconductor fabrication processes are applied to chemical sensor fabrication, function in a manner similar to a measuring probe, identifying a specific component and determining its concentration within the medium. The importance of integrated sensors has been increasingly recognized with the development of technology and science, as miniaturization of sensors offers general advantages with respect to batch fabrication and reduction of cost.[2] However, integrated chemical sensors, especially humidity sensors, have not yet been matured as a commercial product in the global market. The reason for this is that commercial humidity sensors apply polymer materials with a dip-coating or spin coating method as a sensing layer. However, polymer materials cannot withstand the high temperature required to make on-chip microsensors on a semiconductor substrate such as silicon. In addition, the polymer layer of the humidity sensors exhibits varying degrees of sensitivity to identical external influences due to hysteresis and swelling. The aging of this layer can also lead to data errors in the humidity signals.[3,4]

In this study, an integrated humidity sensor system using analog mixed CMOS technology was fabricated with an operational amplifier for signal processing. Furthermore, carbon nitride film has been applied as a new humidity sensing material.

2. DESIGN AND FABRICATION OF THE MICRO HUMIDITY SENSOR SYSTEM

The sensor system is designed by 0.8 um analog mixed CMOS technology with a subsequent post-process. The chip size is 2×4 mm^2 with 28 pins. The system consists of a high input Z amplifier with three operational amplifiers (Op-amp A), an independent operational amplifier (Op-amp B), two Wheatstone-bridge MOSFET sensors (Sensors A and B), and one Wheatstone-bridge resistive sensor (Sensor C). Both nMOS and pMOS have a W/L ratio of $60 \times 3/8$. The amplifier block and the sensor blocks are electrically isolated to reduce unexpected noise, as shown in Fig. 1.

The two stage CMOS Op amp consists of a differential input stage, a second gain stage, and an output buffer. NMOS forms an input differential pair and pMOS forms an active load. The differential input stage is biased by a current mirror in which the reference current is determined by an internal resistor connected to an adjustable external resistor. Figure 2 shows the layout of the micro sensor system. Three metal rings and pads serve as a guard ring protecting against electrical noise as well as cracks and other damage, and also as a heat sink.

*Corresponding author: sensors@kyungnam.ac.kr

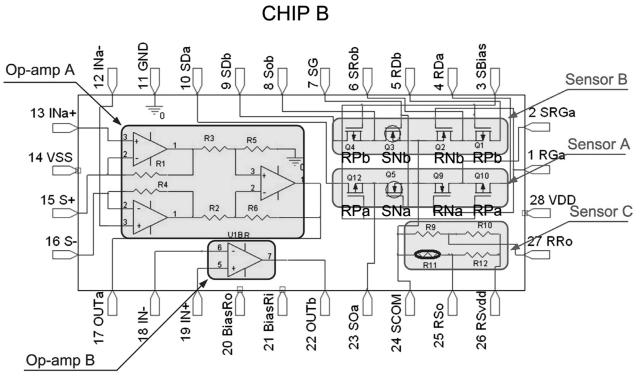

Fig. 1. Schematic view of designed chip.

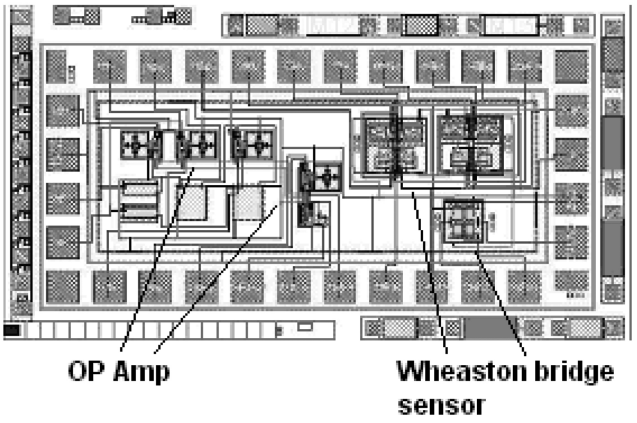

Fig. 2. Layout and inside block of micro sensor system.

The layout of the micro-humidity sensor system is shown in Fig. 3. Each function block in the operational amplifier is separated by a well and metal guard rings. Input lines are given to a twisted pair by two metal layers, as this is a particularly effective and simple way of reducing both magnetic and capacitive interference pickup. Twisting the wires tends to ensure a homogeneous distribution of capacitances. Feedback capacitance of 5 pF is designed near the amplifier block. The common centroid placement design and dummy poly rings are employed to reduce mismatch from over etching and electrical noise. The differential type FET configuration consists of one sensing FET and three reference FETs. The reference transistors are applied to eliminate the unwanted effects from factors such as temperature, other gases, and electrical noise. The differential signal from the sensor FET and reference FETs is transmitted to the amplifier block. The fabrication is based on 0.8 μm CMOS technology, which contains two poly, two metal, and a twin well process. For the formation of sensing materials on the gate layer, plasma etching is performed on each gate along with a trench.[5] Sensing materials are deposited by a reactive RF magnetron sputtering system with DC bias and patterned by a lift-off technique. A carbon nitride film is applied as a new humidity sensing material.[6] To fulfill the requirement of a differential sensor, a gas permeable gold layer is deposited only on the gate region of the sensing transistor.[7,8] The photo resist for passivation is coated on the gate area of reference FETs to protect against reaction with gas. The resistive sensor consists of one sensing resister and three references with a Wheatstone-bridge configuration using the first poly layer. One interdigitated electrode (IDE) pair is opened to sense the water molecules, and the other three references are passivated by a thick photo resist. A N-well is formed under the Wheatstone-bridge configuration for isolation from other devices. The width, length, and spacing of the IDE are 2.80 μm, 58.8 μm, and 1.2 μm, respectively, and each has 6 fingers.

The layout of the two n-channel humidity sensing FET (HUSFET) is shown in Fig. 4. In this parallel connection, HUSFETs operate as a single HUSFET with a width equal to the sum of the individual HUSFET's widths, having equal lengths. The drain and source areas are shared with adjacent HUSFETs. Two benefits are achieved with this layout: (1) smaller layout size and (2) reduction of source and drain depletion capacitances. The second benefit is important in analog circuit design or in output driver design where latch-

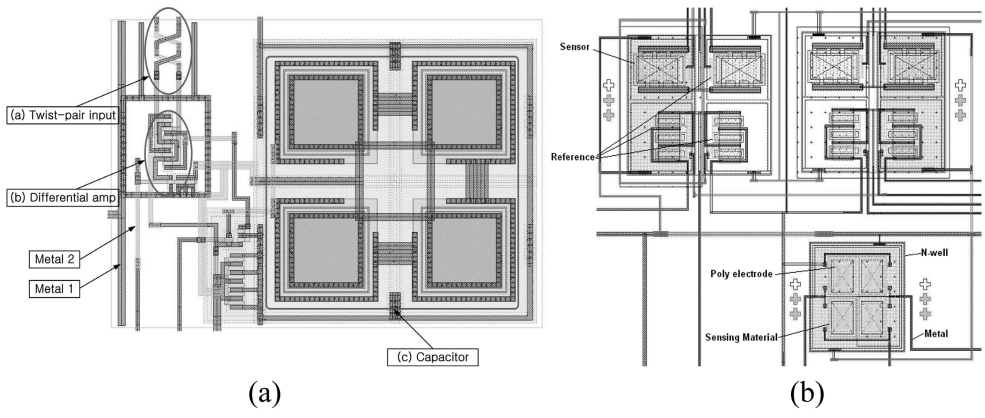

Fig. 3. Layout of micro sensor system; (a) differential operational amplifier and (b) micro humidity sensors.

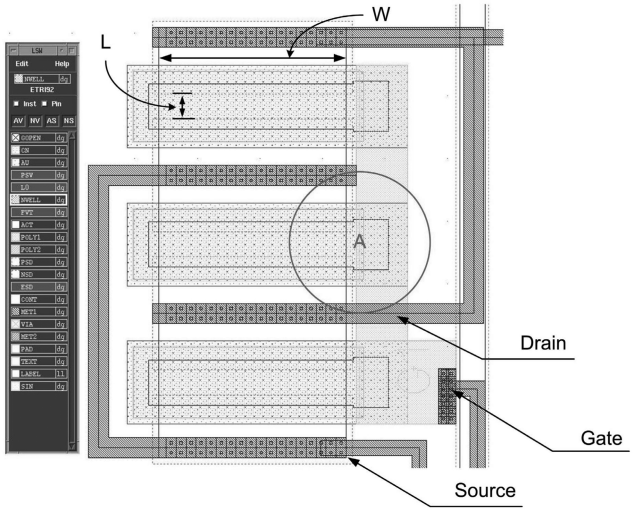

Fig. 4. N-channel HUSFET with shared drain and source.

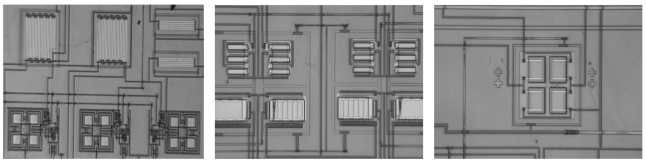

Fig. 5. Photographs of fabricated micro humidity sensor system; (a) operational amplifier, (b) FET sensor and (c) resistive sensor.

up is a concern. A well bulk contact serves as a back-gate for the HUSFETs, but is not explicitly shown in Fig. 4.

Photographs of the fabricated micro-humidity sensor system are shown in Fig. 5.

3. RESULTS AND DISCUSSION

A two stage CMOS Op amp is designed using Hspice simulator for sensor measurement and signal amplification on a single chip. It consists of a differential input stage, a second gain stage, and an output buffer, as shown in Fig. 6. Frequency compensation is necessary for close-loop stability due to a negative-feedback connection. The simplest frequency compensation technique employs the Miller effect by connecting a compensation capacitor C_o across the high-gain stage. NMOSFETs M_1 and M_2 provide the input differential pair, and PMOSFETs M_3 and M_4 provide the active load in Fig. 6. The differential input stage is biased by the current mirrors M_5 and M_8, in which the reference current is determined by the internal resistor connected with an adjustable external resistor (circle A). The second stage, which is the output stage, consists of the common source-connected NMOSFET M_7. Transistor M_8 provides the bias current for M_7 and acts as the active load. An internal compensation capacitor (circle B) and transistor M_9 are included for stability. A bias circuit is designed for stable transconductance,

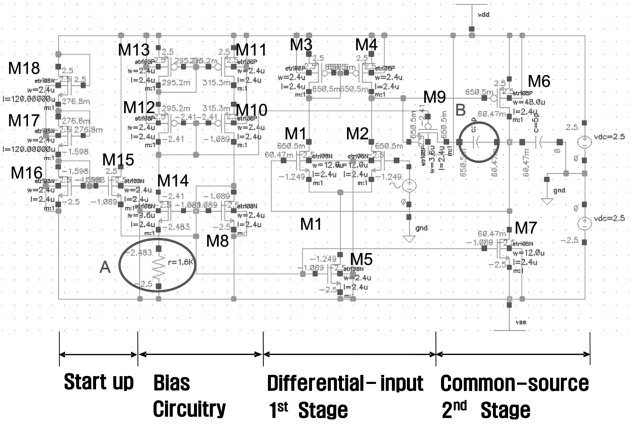

Fig. 6. Circuits of two-stage CMOS operational amplifier with robust bias.

which is matched to the conductance of the bias resistor. Therefore, the transistor transconductance is independent of the power-supply voltage, as well as process and temperature variation. To prevent the zero-current state in the bias circuit, a start-up circuit is included.

The AC response of open loop gain in the operational amplifier is expressed[9]:

$$A_{OL}(f) = \frac{A_O}{1 + j\frac{f}{f_{PD}}} \quad (1)$$

where A_o is the low-frequency open-loop gain and f_{DP} is the dominant-pole frequency. The unity-gain bandwidth is written as

$$f_T = f_{DP}A_O \quad (2)$$

and is also called the gain-bandwidth product. The open loop gain A_0 is about 85 dB and the dominant-pole frequency f_{DP} is about 140 Hz and the unity-gain bandwidth f_T (about 10 MHz) can be obtained at around 1 dB in Fig. 7. Its value is slightly higher than the calculated value from Eq. 2. The specifications of the designed operational amplifier are listed in Table 1.

When water molecules meet the carbon nitride layer through the porous gold layer of FET gate, they are chemisorbed on the available sites of the carbon nitride surface by a dissociative mechanism to form two hydroxyl ions for each water molecule, which possesses a high local charge density and a strong electrostatic field, and the proton reacts with an adjacent surface O^{2-} group to form a second OH^- group, as seen in Fig. 8. Therefore, singly bonded water molecules can form a dipole and reorient freely under an externally applied gate field, resulting in an increase in the dielectric constant. This is also attributed to the threshold voltage and the drain current changes of the FET sensor.[10]

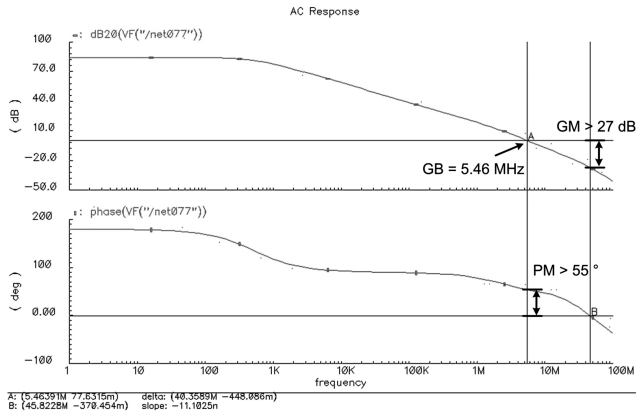

Fig. 7. AC response of unity gain operational amplifier.

Table 1. Specifications of the designed operational amplifier

Technology	0.8 um CMOS
Supply voltage	± 2.5 V
Load capacitance, C_L	5 pF
DC gain	≥ 84 dB
Phase margin	55°
Slew rate	10 V/μs
CMRR	> 80 dB
Settling time	300 ns
Output Swing	± 2 V
Power Consumption	< 0.5 mW

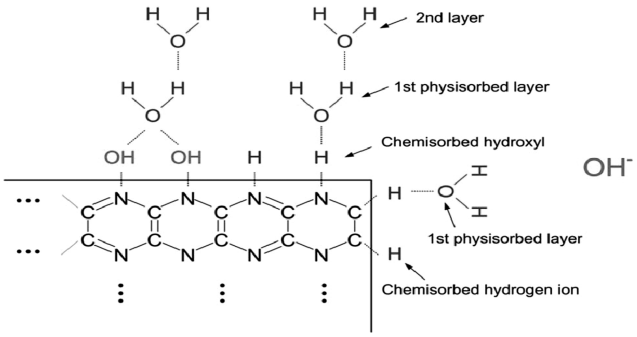

Fig. 8. Mechanism of water molecules adsorption on carbon nitride surface.

Output current characteristics of the HUSFET can be modified by substitution of the total capacitance in the HUSFET gate layer.

$$I_D = \frac{\mu_n Z C_i}{L}\left\{\left(V_G - V_{FB} - 2\phi_F - \frac{1}{2}V_D\right)V_D - \frac{2}{3}\frac{\sqrt{2\varepsilon_s q N_a}}{C_i}\left[(V_D + 2\phi_F)^{2/3} - (2\phi_F)^{2/3}\right]\right\} \quad (3)$$

A porous Au electrode is deposited on a structure of C_3N_4/Si_3N_4/SiO_2/Si in the HUSFET gate layer, and therefore the capacitance per unit area at the inversion state, C_i, can be expressed as

$$C_{in} = C_{ox}C_{sn}/\{((C_{ox} + C_{sn}) + (C_{ox}C_{sn}d_{cn}))/\varepsilon_{ox}\varepsilon_{cn}\} \quad (4)$$

where C_{ox}, C_{sn}, and C_{cn} are the capacitance of unit area in SiO_2, Si_3N_4, and C_3N_4, respectively. d_{cn} is the thickness of the carbon nitride film, ε_{ox} is the relative permittivity of SiO_2, and ε_{cn} is the relative permittivity of CN_x film. When hygroscopic CN_x film is exposed to water molecules, the modified dielectric constant can be given by Looyenga's empirical equation[11]

$$\varepsilon_S = \{\gamma(\varepsilon_w^{1/3} + \varepsilon_{cn}^{1/3}) + \varepsilon_{cn}^{1/3}\}^3 \quad (5)$$

where γ is the fractional volume of water in the carbon nitride film and ε_w is the dielectric constant of water given[12]

$$\varepsilon_w = 78.54\{1 - 4.6\times10^{-4}(T-298) + 8.8\times10^{-6}(T-298)^2\} \quad (6)$$

where T is temperature in Kevin. Shibata *et al*. have reported the calculated γ in a polyimide film.[13]

Figure 9 is the simulated result of Eq. 3, showing the dependence of the dielectric constant on the current-voltage characteristics of the HUSFET. The curves are in fairly good agreement with MOSFET characteristics, despite that the carbon nitride film has been deposited on the gate region. When V_{gs} is -8 V and V_{th} is -9.96 V, the drain current increases from 0.83 mA to 1.14 mA as the dielectric constant of CN_x increases from 4 to 10.

The humidity sensing properties of an n-channel HUSFET are shown in Fig. 10. When the ambient temperature is 25°C

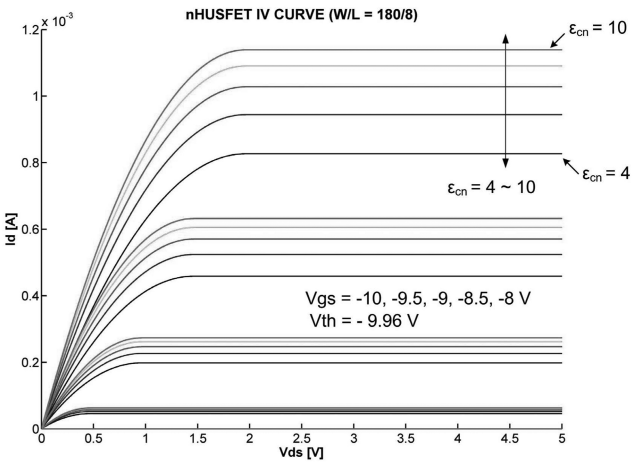

Fig. 9. Simulated I-V curves of HUSFET with dielectric constant changes.

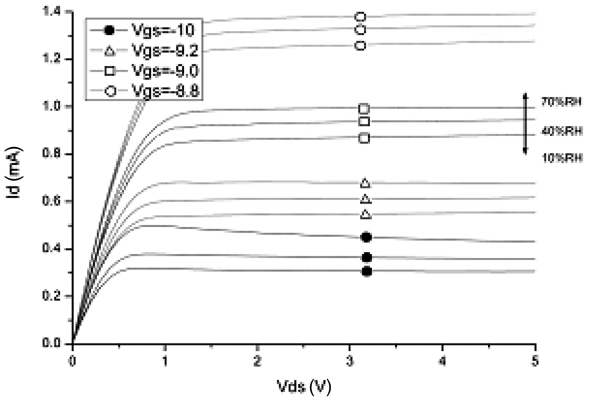

Fig. 10. Humidity sensing characteristics of n-type HUSFET.

and the relative humidity is 20%, the threshold voltage of the n-channel HUSFET (SNa) is about -11.1 V at V_{sb} = 0 V. This value is in good agreement with the simulated results derived from Eq. 3 and presented in Fig. 9. The threshold voltage of the nHUSFET is much lower than that of nMOSFET, because C_i is reduced and the interface charge density Q_i is increased due to the deposition of carbon nitride.

Figure 11 shows the relationship between the drain current and relative humidity of the n-type HUSFET. The gate voltage and source-drain voltage are fixed as V_{gs} = -9.0 V and V_{ds} = 5 V, respectively. As the relative humidity increases from 10 to 70%RH, the drain current increases from 0.88 mA to 0.99 mA. If the sensitivity is defined as $S=dI_D/dRH$, the sensitivity of the n-type HUSFET is 1.83 ßÀ/%RH.

Dynamic changes in the voltage across the sensor, upon exposure to humidity as a function of time, are found to be reproducible and large enough to consider the materials under study, including carbon nitride films, as potential candidates for humidity sensor applications. The response characteristics of the n-type HUSFET are shown in Fig. 12.

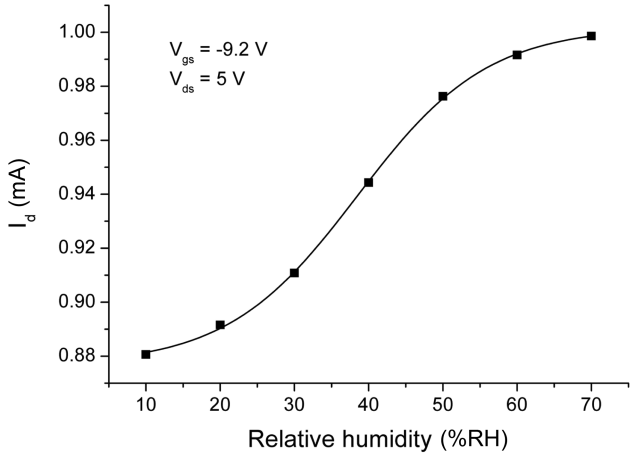

Fig. 11. Drain current vs. relative humidity of n-type HUSFET.

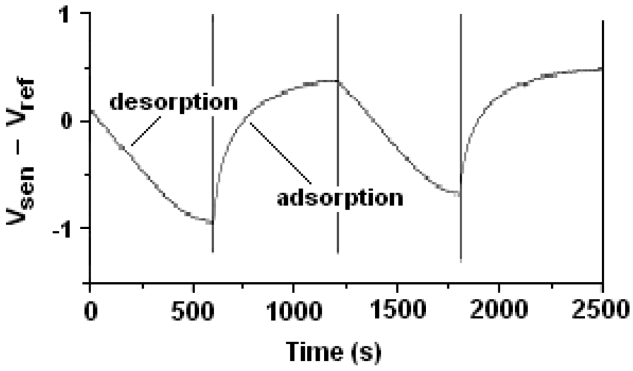

Fig. 12. Response of micro humidity sensor.

When 2,000 sccm humid air and dried air are injected to a constant temperature chamber (25℃) in a period of 600 s, the voltage difference between the sensor and reference is about 1 V_{p-p}. Response and recovery times to achieve 90 % of the final voltage are 500 s and 520 s, respectively.

4. CONCLUSIONS

An integrated multi-sensor system with an operational amplifier was designed and fabricated by a 0.8 μm analog mixed CMOS process. A carbon nitride film was applied for the first time as a humidity sensing material in a FET humidity sensor. The integrated sensor system consists of a Wheatstone bridge FET senor, a Wheatstone bridge resistive sensor, a diode temperature sensor, and an operational amplifier. The fabricated operational amplifier presented DC gain of over 85 dB, unity gain bandwidth of about 10 MHz, and a slew rate in excess of 10 V/uS, respectively. The drain current of an n-type HUSFET increased from 0.88 mA to 0.99 mA as the relative humidity was increased from 10 %RH to 70 %RH. The voltage difference of the sensor and reference in the sensor is about 1 V_{p-p}. The response and recovery times of the gas sensor are 500 s and 520 s at 25, respectively.

ACKNOWLEDGEMENT

This work was supported by Kyungnam University Foundation Grant 2007.

REFERENCES

1. H. Meixner, and R. Jones, *Sensors in Micro- and Nanotechnology, Sensors Vol.* 8, p. 3, VCH, Weinheim (1995).
2. Z. Rittersma, *Sensors and Actuator* **A 96**, 196 (2002).
3. M. Matsuguchi, Y. Sadaoka, Y. Sakai, T. Kuroiwa, and A. Ito, *J. Electrochem. Soc*. **138**, 1862 (1991).
4. M. Matsuguchi, T. Kuroiwa, T. Miyagishi, S. Suzuki, T. Ogura, and Y. Sakai, *Sensors and Actuators* **B52**, 53 (1998).

5. T. S. Kim , H. Y. Yang , S. S. Choi , T. S. Jeong , S. K. Kang , and K. H. Shim, *Electron. Mater. Lett*. **5**, 43 (2009).
6. S. P. Lee, *Electron. Mater. Lett.* **5**, 1 (2009).
7. S. P. Lee and K. J. Park, *Sensors and Actuators* **B35-36**, 80 (1996).
8. S. Y. Kim, J. G. Lee, C. W. Chang, and S. P. Lee, *J. of the Korean Sensors Soc.* **16**, 97 (2007).
9. S. P. Lee, J. G. Lee, and S. Chowdhury, *Sensors* **8**, 2662 (2008).
10. S. Martinoia, G. Massobrio, and L. Lorenzelli, *Sensors and Actuators* **B108**, 14 (2005).
11. D. Schubert, and J. Nevin, *IEEE Trans Electron Devices* **ED-32**, 1220 (1985).
12. J. Hasted, *Aqueous Dielectrics*, p. 37-38, Chapman and Hall, London (1973).
13. H. Shibata, M. Ito, A. Asakursa, and K. Watanabe, *IEEE Trans Instrum. Meas.* **45**, 564 (1986).